

1 | Physics at LHC

The Large Hadron Collider (LHC) [Evans'2008] is a hadron and heavy ion accelerator and collider installed near Geneva in a 27 km long tunnel at the depth of about 100m constructed between 1984 and 1989 for the LEP machine.

The project was approved by CERN (European Organization for Nuclear Research) Council in December 1994 and designed to overcome in terms of center of mass energy and luminosity the existing accelerators such as the Tevatron at Fermilab and LEP (Large Electron Positron) at CERN.

The first beams were accelerated to 7 TeV in 2010/2011 and 8 TeV in 2012. In 2015 LHC reached the nominal energy of 13 TeV and in 2018 an instantaneous luminosity of $2 \times 10^{34} \text{cm}^{-2} \text{s}^{-1}$ well above the designed value.

In 2024 the machine and the detectors will undergo a long list of upgrades with the final goal to increase the total amount of integrated luminosity by a factor of 10 by 2035.

This chapter will briefly introduce Quantum Chromodynamics (QCD), which is the theory used to describe a hadron scattering, its lagrangian and the associated Feynman rules followed by a summary of the LHC apparatus. Finally, a description of the role of computer simulations in today's environment and its drawbacks are discussed in Section 1.3.

1.1 QCD background

Quantum Chromodynamics is the theory that describes the strong interactions. It is a non-Abelian Gauge theory with Gauge group $SU(3)$, the success of this theory is due to the agreement with the phenomenon of asymptotic freedom.

This effect enables the possibility of calculation of cross sections in high energy physics through perturbation theory, but even in this case contributions from lower energy scale are important and need to be considered suggesting a potential hole in the predictive power of the theory.

However, thanks to the factorization theorem, it is possible to separate the perturbative contribution at short distance from the non-perturbative contributions

at long distance and hence restore the possibility of making predictions with both contributions.

QCD lagrangian

In order to write the QCD lagrangian let us define a fermionic quantum field with a color triplet:

$$\psi(x) = \begin{pmatrix} \psi_1(x) \\ \psi_2(x) \\ \psi_3(x) \end{pmatrix} \quad (1.1)$$

QCD is a non-Abelian Gauge theory, also called Yang-Mills theory, in which the symmetry group is SU(3). Moreover, the global symmetry of SU(3) is promoted to a local symmetry, this means that the field $\psi(x)$ transform as $\psi(x) \rightarrow U(x)\psi(x)$ where $U(x) = e^{ig\lambda_a(x)T^a/2}$ and g is a dimensionless coupling constant. The T^a 's are hermitian and traceless 3 x 3 matrices and they generate the Lie algebra with commutation rules given by:

$$[T^a, T^b] = if^{abc}T_c \quad (1.2)$$

where the structure constants f^{abc} are real and antisymmetric.

Assuming the local symmetry of the group, it is necessary to define a new Gauge field and it's transformation rule in order to ensure that the derivative term of the field transform like the field itself. To do so, we define the Gauge field A_μ^a and the covariant derivative $D_\mu = (\partial_\mu - igT_a A_\mu^a)$, with the transformation rule:

$$A_\mu \rightarrow U(x)(A_\mu - \frac{i}{g}\partial_\mu)U^\dagger(x) \quad (1.3)$$

the derivative term transform as $D_\mu\psi(x) \rightarrow U(x)D_\mu\psi(x)$, where A_μ is a shorthand of $A_\mu^a T^a$. The T^a are written in the adjoint representation in which the index a runs from 1 to 8, this allows to interpret the fields A_μ^a as eight gluons mediators of the strong force.

Summarizing, the full QCD lagrangian with the kinetic terms for $\psi(x)$ and $A_\mu(x)$ plus the mass terms can be written as:

$$\mathcal{L} = -\frac{1}{4}F_{\mu\nu}^a F^{a\mu\nu} + \sum_q \bar{\psi}_k^j (i\not{D}_j^k - m\delta_j^k)\psi_k \quad (1.4)$$

where the sum is carried over the number of quarks and $F_{\mu\nu}^a = \partial_\mu A_\nu^a - \partial_\nu A_\mu^a + gf^{abc}A_\mu^b A_\nu^c$ is the gauge field strength tensor. In order to correctly quantize the

theory it's necessary to use the Fadeev-Popov method which introduce other virtual particles called 'ghosts' adding to the previous lagrangian the terms:

$$\mathcal{L}_{ghost} = \partial_\mu \bar{c}^a \partial^\mu c^a + g f^{abc} (\partial^\mu \bar{c}^a) A_\mu^b c^c \quad (1.5)$$

Writing explicitly the gauge strength tensor and the covariant derivative it is possible to derive the Feynman rules of QCD included in Appendix A.

Factorization theorem

One of the major successes of QCD theory is that it can describe asymptotic freedom. Naively, the interaction between particles becomes asymptotically zero at increasing energy thus, even if low energy contributions cannot be neglected, it is possible to obtain a perturbative expansion at the order of the QCD coupling constant α_s for a high energy hadron scattering. Given to ability to calculate the cross section for a hard scattering process with a perturbative expansion, the factorization theorem accounts for the contributions at low energy with multiplying factors to the hard term that depend on all the partons included in the process and their fraction of the total energy.

For the interest of LHC, consider a high energy scattering between two hadrons, namely two protons $p(P_a)$ and $p(P_b)$. Suppose that the hard scattering involves two partons a and b with longitudinal energy fraction x_a and x_b since the momentum fractions of the hadron constituents cannot be calculated with perturbative QCD, a function it is associated with the probability of finding the constituents a or b with longitudinal momentum fraction x_a or x_b . These function $f_i(x_i)$ are universal for a given hadron and are called parton distribution functions.

Applying the factorization theorem and pQCD to a deep inelastic scattering the cross section $\sigma(p(P_1) + p(P_2) \rightarrow Y + X)$ at Leading Order is given by:

$$\sigma(p(P_a) + p(P_b) \rightarrow Y + X) = \int_0^1 dx_a \int_0^1 dx_b \sum_{a,b} f_a(x_a) f_b(x_b) \cdot \sigma_{ab \rightarrow Y}(x_a, x_b) \quad (1.6)$$

where Y and $\sigma_{ab \rightarrow Y}$ are, respectively, the final state and the cross section of the hard scattering process, X is any possible hadronic final state and the sum is carried over all species of quarks and antiquarks.

1.2 *pp collisions at LHC*

At the LHC the collision of beams doesn't involve single particles, indeed the beam is composed of about 10^{11} protons squeezed in bunches of size $\sim 17 \mu\text{m}$ in the transverse direction and $\sim 8 \text{ cm}$ in the beam direction. This means that at the interaction point different types of collisions could happen:

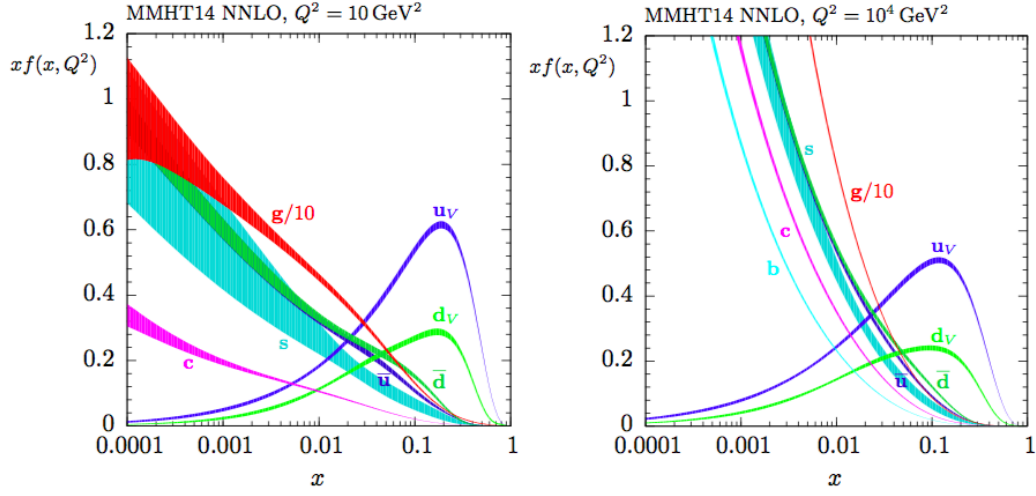


Figura 1.1: Parton Distribution Functions (PDFs) computed for $\mu^2 = 10^2 \text{ GeV}^2$ and $\mu^2 = 10^4 \text{ GeV}^2$ from MMHT 2014 PDFs.

- 150 – Soft collisions consisting of initial and final state radiation and soft parton
151 interactions with typically low transferred momentum. The method used to
152 study these collisions is with non-perturbative QCD and the measurement of
153 these effects is fundamental for real events.
- 154 – Hard collisions are rarer events in which the fundamental constituents of
155 protons come to light and are the interesting ones in experiments. They are
156 described by perturbative QCD and characterized by short distance collision
157 and high transferred momentum enabling them to produce new particles.

158 As described in Section 1.1 an hard inelastic collision could be interpreted as
159 a scattering between two partons (quarks or gluons) each one carrying a fraction
160 x_i of the total momentum of the particles. Therefore the center of mass energy
161 \sqrt{s} during the collision of two partons a, b is a fraction of the total centre-of-mass
162 energy \sqrt{s} :

$$\sqrt{s} = \sqrt{x_a x_b s} \quad (1.7)$$

163 where x_a, x_b are the fractions of the total momentum carried by the partons.

164 The cross-section for a hard scattering collision is given by Eq. 1.6 where a
165 proper treatment of the parton distribution functions $f_i(x_i, Q^2)$, $f_j(x_j, Q^2)$ and of
166 the hard scattering cross section $\sigma_{ab \rightarrow Y}(x_a, x_b, Q^2)$ at higher order introduce the
167 dependence on the energy scale Q^2 .

168 Figure 1.3 shows the PDFs for $Q^2 = 10^2 \text{ GeV}^2$ and $Q^2 = 10^4 \text{ GeV}^2$.

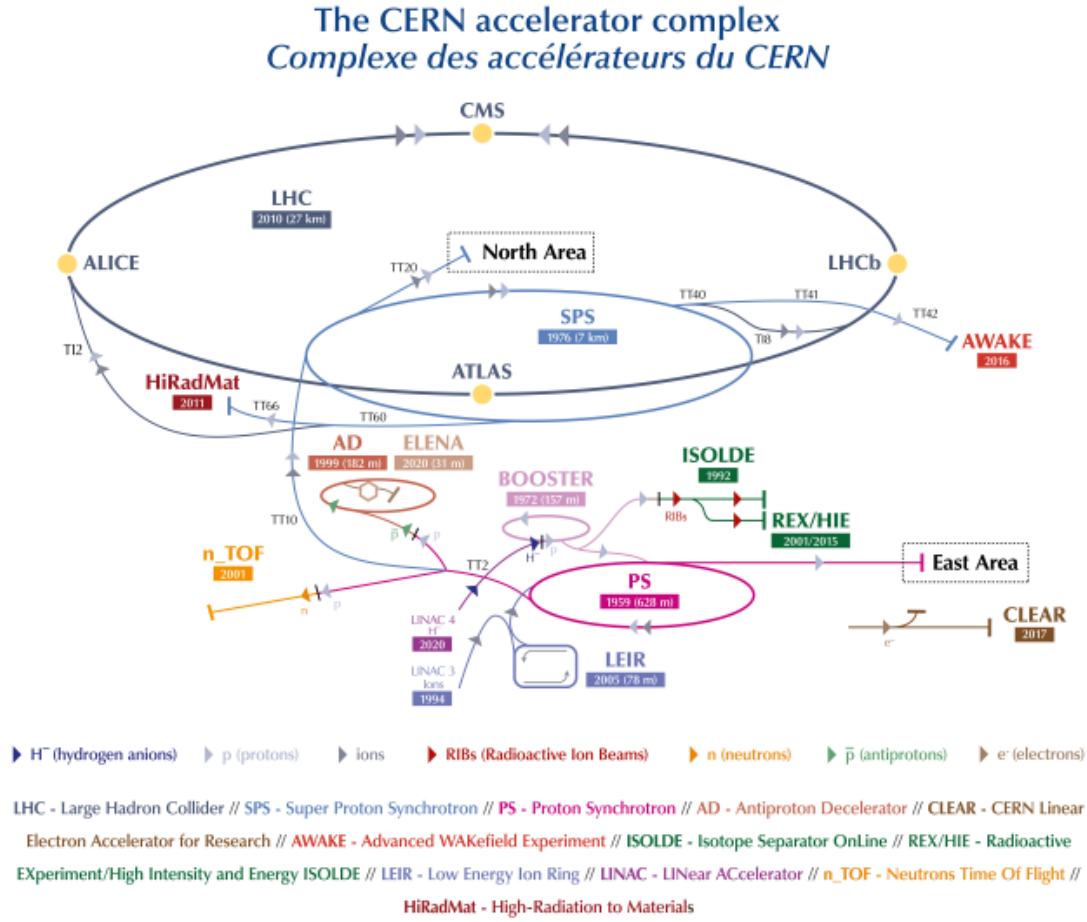


Figure 1.2: Accelerator complex at CERN[Mobs].

LHC structure

To reach the final energy of 6.5 TeV the beams are gradually speeded up by different accelerators as shown in Figure 1.2.

Initially, an electric field separate protons from electrons and then injected into the accelerators chain:

- a linear accelerator (LINAC) speeds up protons up to 50 MeV;
- the beam is then injected into the Proton Synchrotron Booster (PSB), which accelerates the protons up to 1.4 GeV;
- then the Proton Synchrotron (PS) pushes the beam up to 25 GeV;

– protons are then injected in the Super Proton Synchrotron (SPS) where they are accelerated up to 450 GeV.

Finally, the protons are injected in LHC using two beam pipes in which the two beams circulate clockwise and anti-clockwise directions and then accelerated to the nominal $\frac{\sqrt{s}}{2}$ energy. It takes 4 minutes and 20 seconds to inject a beam into LHC and about 20 minutes for protons to reach their maximum energy of 6.5 TeV.

The LHC relies on more than 1000 superconducting dipole magnets to bend the beam in the ring. This magnets system is cooled to a temperature below 2 K using superfluid helium and produces a field of 8.4 T. Moreover, to ensure beam stability, quadrupole, sextupoles, octupoles, and decupoles magnets are installed at different points of the beam pipe.

1.3 The role of simulations at LHC

Simulations are a key component for studies at LHC, indeed they are the junction point between the theoretic model and the real experiment.

The full simulation of events can be summarized in three steps:

- Generation: an event generator produce the particles of the scattering process to study, e.g. proton-proton parton scattering into two top quarks;
- Detector interaction: this step simulates the interaction between the produced particles and the detector material;
- Digitization: finally, a simulation is needed to reproduce the measured signal and to obtain data in the same form of real events. Moreover, this step accounts for the instrumental effects like noises and thresholds.

The results obtained from a full simulation provide answers to a range of different questions from the discovery of new physics, like the number of events needed to distinguish a particular channel from the background, to the deterioration state of detector components. In this environment, Machine Learning techniques already are ubiquitous in a vast range of applications from discrimination from signal and background to objects reconstruction, and with the upcoming of more performant algorithms and hardware, the expectations are that their usage will be extended.

One of the major issues for LHC in the next years will be the CPU and storage capabilities, especially during the HL-LHC era. As Figure 1.3 shows, the baseline prediction of the majority of the CPU usage for ATLAS and CMS is associated with simulations using Monte Carlo techniques. This approach can be really slow and CPU expensive and looking forward into the next years the typical increase in resource available will not be enough to account for the statistic required by LHC.

1.3. THE ROLE OF SIMULATIONS ~~THE~~ROLE OF SIMULATIONS AT LHC

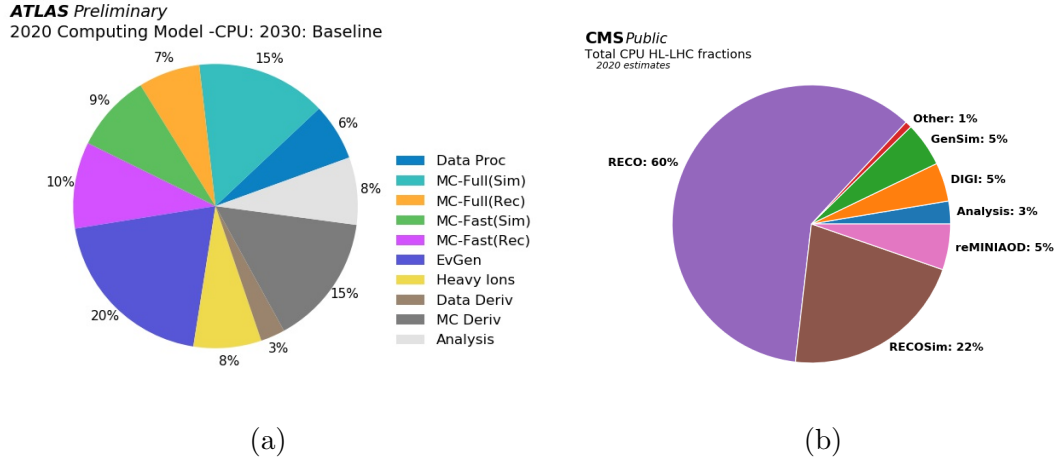


Figure 1.3: Snapshot of projected CPU resources required by ATLAS (a) and CMS (b) in 2030, by computational task. [**cpu-atlas**]

The ATLAS and CMS collaborations forecast that during the HL-LHC era, where the average number of collisions per event will be ~ 200 , the CPU consumption will be ~ 5 times greater than the available resources. However, the LHCb collaboration reports that already in the next years that limit will be exceeded, both forecasts are shown in Figure 1.4.

To overcome this problem different projects regarding fast simulations are in development nowadays, indeed one of the key tools could be the implementation of new Machine Learning based generative techniques.

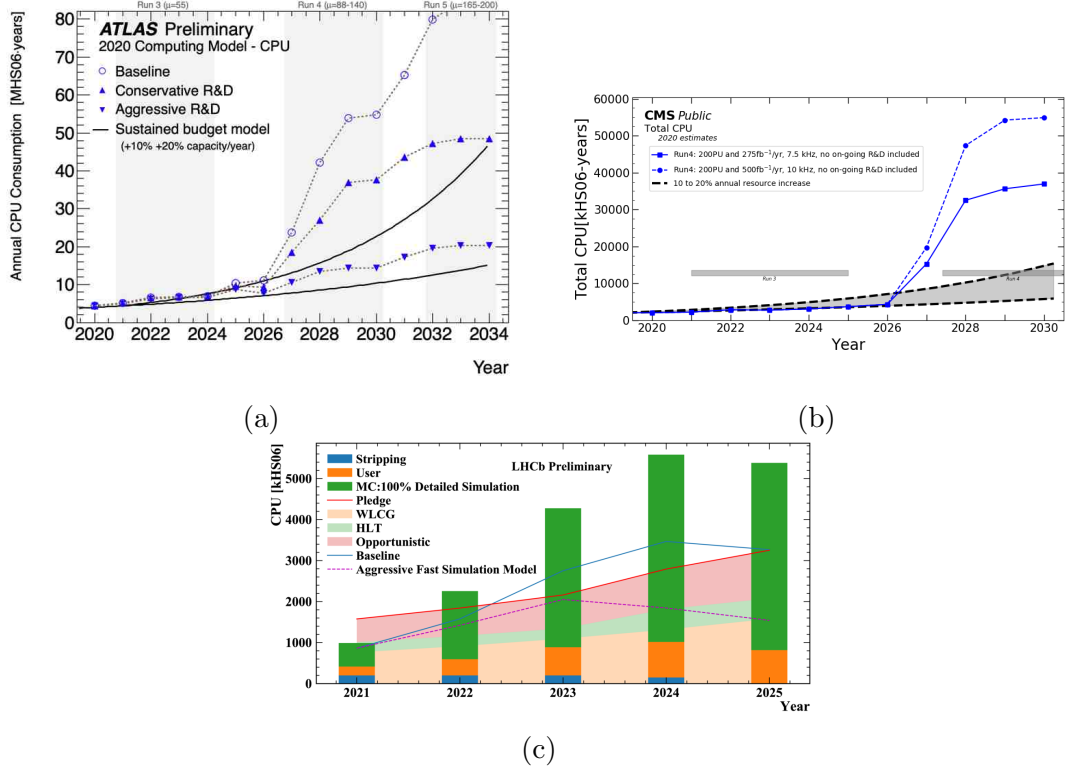


Figura 1.4: (a) Projected CPU requirements (in kilo-HEPSpec06 years) of ATLAS between 2020 and 2034 based on 2020 assessment. Three scenarios are shown, corresponding to an ambitious (“aggressive”), modest (“conservative”) and minimal (“baseline”) development program. The black lines indicate annual improvements of 10% and 20% in the computational capacity of new hardware for a given cost, assuming a sustained level of annual investment. The blue dots with the brown lines represent the 3 ATLAS scenarios following the present LHC schedule. [cpu-atlas] (b) CPU time requirements (in kilo-HEPSpec06 years) estimated to be required annually for CMS processing and analysis needs. The scenarios considered are 275 fb^{-1} per year of 7.5 kHz of data collected (solid line) and 500 fb^{-1} per year of 10 kHz of data collected (dashed line) both without R&D predictions. (c) Estimated CPU usage for the LHCb experiment from 2021 through 2025 (in kilo-HEPSpec06 years). The bars give the total CPU usage expected, composed of stripping jobs (blue), all estimated user jobs (orange) and simulation production (green). The green bars here assume only fully detailed simulation to be run. [cpu-lhcb]